

COUPLED NONLINEAR OSCILLATORS:
METAMORPHOSES OF AMPLITUDE PROFILES.
THE CASE OF THE APPROXIMATE
EFFECTIVE EQUATION

JAN KYZIOŁ

Kielce University of Technology
Department of Mechatronics and Mechanical Engineering
Al. 1000-lecia Państwa Polskiego 7, 25-314 Kielce, Poland

ANDRZEJ OKNIŃSKI

Kielce University of Technology
Physics Division, Department of Management and Computer Modelling
Al. 1000-lecia Państwa Polskiego 7, 25-314 Kielce, Poland

(Received August 29, 2011)

We study dynamics of two coupled periodically driven oscillators. Important example of such a system is a dynamic vibration absorber which consists of a small mass attached to the primary vibrating system of a large mass. Periodic solutions of the approximate effective equation derived in our earlier work are determined within the Krylov–Bogoliubov–Mitropolsky (KBM) approach used to compute the amplitude profiles $A(\Omega)$. Dependence of the amplitude A of nonlinear resonances on the frequency Ω is much more complicated than in the case of one Duffing oscillator and hence new nonlinear phenomena are possible. In the present paper we study metamorphoses of the function $A(\Omega)$ induced by changes of the control parameters near a singular point of this function. It follows that dynamics can be controlled in the neighbourhood of a singular point.

DOI:10.5506/APhysPolB.42.2063

PACS numbers: 05.45.Xt, 02.40.Xx

1. Introduction

Coupled oscillators play important role in many scientific fields, *e.g.* biology, electronics, and mechanics, see [1, 2, 3, 4, 5] and references therein. In this paper we analyse two coupled oscillators, one of which is driven by an external periodic force. Important example of such system is a dynamic

vibration absorber which consists of a mass m_2 , attached to the primary vibrating system of mass m_1 [6, 7]. Equations describing dynamics of such system are of form

$$\left. \begin{aligned} m_1 \ddot{x}_1 - V_1(\dot{x}_1) - R_1(x_1) + V_2(\dot{x}_2 - \dot{x}_1) + R_2(x_2 - x_1) &= f \cos(\omega t) \\ m_2 \ddot{x}_2 - V_2(\dot{x}_2 - \dot{x}_1) - R_2(x_2 - x_1) &= 0 \end{aligned} \right\}, \quad (1.1)$$

where V_1 , R_1 and V_2 , R_2 represent (nonlinear) force of internal friction and (nonlinear) elastic restoring force for mass m_1 and mass m_2 , respectively. In the present paper we do not assume that the ratio m_2/m_1 is small.

In the present paper we shall consider a simplified model:

$$R_1(x_1) = -\alpha_1 x_1, \quad V_1(\dot{x}_1) = -\nu_1 \dot{x}_1. \quad (1.2)$$

Dynamics of coupled periodically driven oscillators is very complicated [2, 3, 5]. We simplified the set of equations (1.1), (1.2) by reducing it to the problem of motion of two independent oscillators. More precisely, we derived the exact fourth-order nonlinear equation for internal motion as well as approximate second-order effective equation in [8]. Moreover, applying the Krylov–Bogoliubov–Mitropolsky method to these equations we have computed the corresponding nonlinear resonances (*cf.* [8] for the case of the effective equation). Dependence of the amplitude A of nonlinear resonances on the frequency ω is much more complicated than in the case of Duffing oscillator and hence new nonlinear phenomena are possible. In the present paper we study metamorphoses of the function $A(\omega)$ induced by changes of the control parameters.

The paper is organized as follows. In the next section derivation of the exact fourth-order equation for the internal motion and approximate second-order effective equations in non-dimensional form are presented. In Sec. 3 metamorphoses of amplitude profiles determined within the Krylov–Bogoliubov–Mitropolsky approach for the approximate second-order effective equation are studied and the case of the standard Duffing equation is presented as well. More exactly, theory of algebraic curves is used to compute singular points on effective equation amplitude profiles — metamorphoses of amplitude profiles occur in neighbourhoods of such points. In Sec. 4 examples of analytical and numerical computations are presented for the effective equation. Our results are summarized and perspectives of further studies are described in the last section.

2. Exact equation for internal motion and its approximations

In new variables, $x \equiv x_1$, $y \equiv x_2 - x_1$, equations (1.1), (1.2) can be written as

$$\left. \begin{aligned} m\ddot{x} + \nu\dot{x} + \alpha x + V_e(\dot{y}) + R_e(y) &= f \cos(\omega t) \\ m_e(\ddot{x} + \ddot{y}) - V_e(\dot{y}) - R_e(y) &= 0 \end{aligned} \right\}, \tag{2.1}$$

where $m \equiv m_1$, $m_e \equiv m_2$, $\nu \equiv \nu_1$, $\alpha \equiv \alpha_1$, $V_e \equiv V_2$, $R_e \equiv R_2$.

Adding equations (2.1) we obtain important relation between variables x and y

$$M\ddot{x} + \nu_1\dot{x} + \alpha_1x + m_e\ddot{y} = f \cos(\omega t), \tag{2.2}$$

where $M = m + m_e$.

We can eliminate variable x in (2.1) to obtain the following exact equation for relative motion

$$\left(M \frac{d^2}{dt^2} + \nu \frac{d}{dt} + \alpha \right) (\mu \ddot{y} - V_e(\dot{y}) - R_e(y)) + \lambda m_e \left(\nu \frac{d}{dt} + \alpha \right) \ddot{y} = F \cos(\omega t), \tag{2.3}$$

where $F = m_e \omega^2 f$, $\mu = mm_e/M$ and $\lambda = m_e/M$ is a nondimensional parameter. Equations (2.3), (2.2) are equivalent to the initial equations (1.1), (1.2) [8].

In the present work we assume

$$R_e(y) = \alpha_e y - \gamma_e y^3, \quad V_e(\dot{y}) = -\nu_e \dot{y}. \tag{2.4}$$

We thus get

$$\begin{aligned} &\left(M \frac{d^2}{dt^2} + \nu \frac{d}{dt} + \alpha \right) \left(\mu \frac{d^2 y}{dt^2} + \nu_e \frac{dy}{dt} - \alpha_e y + \gamma_e y^3 \right) \\ &+ \lambda m_e \left(\nu \frac{d}{dt} + \alpha \right) \frac{d^2 y}{dt^2} = F \cos(\omega t). \end{aligned} \tag{2.5}$$

We shall write Eq. (2.5) in nondimensional form. Introducing nondimensional time τ and rescaling variable y

$$\tau = t\bar{\omega}, \quad z = y \sqrt{\frac{\gamma_e}{\alpha_e}}, \tag{2.6}$$

where

$$\bar{\omega} = \sqrt{\frac{\alpha_e}{\mu}}, \tag{2.7}$$

we get the exact equation for motion of mass m_e

$$\begin{aligned} & \left(\frac{d^2}{d\tau^2} + H \frac{d}{d\tau} + a \right) \left(\frac{d^2 z}{d\tau^2} + h \frac{dz}{d\tau} - z + z^3 \right) \\ & + \kappa \left(H \frac{d}{d\tau} + a \right) \frac{d^2 z}{d\tau^2} = G \frac{\kappa}{\kappa + 1} \Omega^2 \cos(\Omega\tau), \end{aligned} \tag{2.8}$$

where nondimensional constants are given by

$$\begin{aligned} h &= \frac{\nu_e}{\mu\bar{\omega}}, & H &= \frac{\nu}{M\bar{\omega}}, & \Omega &= \frac{\omega}{\bar{\omega}}, \\ G &= \frac{1}{\alpha_e} \sqrt{\frac{\gamma_e}{\alpha_e}} f, & \kappa &= \frac{m_e}{m}, & a &= \frac{\alpha\mu}{\alpha_e M}. \end{aligned} \tag{2.9}$$

We shall consider hierarchy of approximate equations arising from (2.8). For small κ , H , a we can reject the second term on the left in (2.8) to obtain the approximate equation

$$\left(\frac{d^2}{d\tau^2} + H \frac{d}{d\tau} + a \right) \left(\frac{d^2 z}{d\tau^2} + h \frac{dz}{d\tau} - z + z^3 \right) = \gamma \Omega^2 \cos(\Omega\tau) \quad \left(\gamma \equiv G \frac{\kappa}{\kappa + 1} \right) \tag{2.10}$$

which can be integrated partly to yield the effective equation

$$\frac{d^2 z}{d\tau^2} + h \frac{dz}{d\tau} - z + z^3 = -\gamma \frac{\Omega^2}{\sqrt{(\Omega^2 - a)^2 + H^2 \Omega^2}} \cos(\Omega\tau + \delta), \tag{2.11}$$

for appropriate δ , where transient states has been omitted [8] (indeed, $\left(\frac{d^2}{d\tau^2} + H \frac{d}{d\tau} + a \right) g(\tau) = \gamma \Omega^2 \cos(\Omega\tau)$ for $g(\tau) = -\gamma \Omega^2 \frac{\cos(\Omega\tau + \delta)}{\sqrt{(\Omega^2 - a)^2 + H^2 \Omega^2}} +$ transient terms). And finally, for $H = 0$, $a = 0$ we get the Duffing equation

$$\frac{d^2 z}{d\tau^2} + h \frac{dz}{d\tau} - z + z^3 = -\gamma \cos(\Omega\tau + \delta). \tag{2.12}$$

3. Metamorphoses of the amplitude profiles

We applied the Krylov–Bogoliubov–Mitropolsky perturbation approach [9, 10], working in the spirit of Ref. [4], to the effective equation (2.11) obtaining for the 1 : 1 resonance the following amplitude profile [8]

$$A_{\text{eff}} = \frac{\gamma \Omega^2}{\sqrt{\left(h^2 \Omega^2 + \left(1 + \Omega^2 - \frac{3}{4} A_{\text{eff}}^2 \right)^2 \right) \left((\Omega^2 - a)^2 + H^2 \Omega^2 \right)}}. \tag{3.1}$$

Now, for $H = 0$, $a = 0$ we obtain the amplitude profile for the Duffing equation (2.12)

$$A_D = \frac{\gamma}{\sqrt{\left(h^2\Omega^2 + \left(1 + \Omega^2 - \frac{3}{4}A_D^2\right)^2\right)}}. \tag{3.2}$$

It is well known that dependence of the function A_D , cf. (3.2), on control parameters γ, h is rather simple. On the other hand, dependence of the amplitude profile $A_{\text{eff}}(\Omega)$ on control parameters γ, h, a, H is more complicated and thus $A_{\text{eff}}(\Omega)$ can describe new nonlinear phenomena. In the next section we shall study possible metamorphoses of A_D, A_{eff} induced by changes of control parameters. The more complicated case of the fourth-order exact equation (2.8) will be treated elsewhere.

Equations (3.2), (3.1) define the corresponding amplitude profiles implicitly. Such amplitude profiles can be classified as planar algebraic curves. Firstly, we shall collect useful theorems on implicit functions which will be used below.

Let us write equations (3.1), (3.2) as $L_e(Y_e, X) = 0$ and $L_D(Y_D, X) = 0$, respectively, where $X \equiv \Omega^2, Y \equiv A^2$

$$\left(h^2X + \left(1 + X - \frac{3}{4}Y_e\right)^2\right) \left((X - a)^2 + H^2X\right) Y_e - \gamma^2 X^2 = 0, \tag{3.3}$$

$$\left(h^2X + \left(1 + X - \frac{3}{4}Y_D\right)^2\right) Y_D - \gamma^2 = 0. \tag{3.4}$$

It follows from general theory of implicit functions [11,12] that conditions for critical points of $Y(X)$ read

$$L(Y, X) = 0, \quad \frac{\partial L(Y, X)}{\partial X} = 0 \quad \left(\frac{\partial L(Y, X)}{\partial Y} \neq 0\right). \tag{3.5}$$

Moreover, critical points of the inverse function $X(Y)$ are given by

$$L(Y, X) = 0, \quad \frac{\partial L(Y, X)}{\partial Y} = 0 \quad \left(\frac{\partial L(Y, X)}{\partial X} \neq 0\right). \tag{3.6}$$

It may happen that in some points (X_0, Y_0) we have

$$L(Y, X) = 0, \quad \frac{\partial L(Y, X)}{\partial X} = 0, \quad \frac{\partial L(Y, X)}{\partial Y} = 0. \tag{3.7}$$

Such points are referred to as singular points of algebraic curve $L(Y, X) = 0$ because they are in some sense exceptional.

3.1. *The case of the Duffing equation*

Singular points of the algebraic curve defined by (3.4) are given by

$$\frac{\partial L_D}{\partial X} = 0, \tag{3.8}$$

$$\frac{\partial L_D}{\partial Y} = 0. \tag{3.9}$$

The set of equations (3.4), (3.8), (3.9) can be written as

$$h^2XY + Y(1 + X - \frac{3}{4}Y)^2 - \gamma^2 = 0, \tag{3.10}$$

$$h^2Y + 2Y + 2YX - \frac{3}{2}Y^2 = 0, \tag{3.11}$$

$$h^2X + 1 + 2X - 3Y + X^2 - 3YX + \frac{27}{16}Y^2 = 0, \tag{3.12}$$

where X, Y are positive.

General solution reads

$$\begin{cases} X = -\frac{1}{2}h^2 - 1 + \frac{3}{4}Y & (Y \neq 0) \\ Y = \frac{1}{6}h^2 + \frac{2}{3} & (h \neq 0) \\ \gamma^2 = -\frac{1}{48}h^6 - \frac{1}{6}h^4 - \frac{1}{3}h^2 \end{cases} . \tag{3.13}$$

It follows that $Y > 0, X < 0$ and $\gamma^2 \leq 0$ and thus the system of equations (3.10), (3.11), (3.12) has no acceptable solutions since we assume that h, γ are real and X, Y are non-negative.

3.2. *The case of the effective equation*

Singular points of the algebraic curve defined by (3.3) are given by equations

$$\frac{\partial L_e}{\partial X} = 0, \tag{3.14}$$

$$\frac{\partial L_e}{\partial Y} = 0. \tag{3.15}$$

It follows from (3.3) and (3.15) that either of equations must hold

$$16X^2 + 16h^2X + 32X + 16 - 48YX - 48Y + 27Y^2 = 0, \tag{3.16}$$

$$(X - a)^2 + H^2X = 0, \tag{3.17}$$

where X, Y are positive.

Let us start with Eq. (3.17). In this case we obtain from (3.3), (3.14) and (3.17) the following rather special solution

$$X = a, \quad H = 0, \quad \gamma = 0, \tag{3.18}$$

where Y, h, a are arbitrary.

Let us now consider more general Eq. (3.16). We can treat X as arbitrary. Then we obtain two solutions for Y

$$Y = \frac{8}{9} + \frac{8}{9}X - \frac{4}{9}\sqrt{1 + 2X + X^2 - 3h^2X}, \tag{3.19}$$

$$Y = \frac{8}{9} + \frac{8}{9}X + \frac{4}{9}\sqrt{1 + 2X + X^2 - 3h^2X}, \tag{3.20}$$

where the inequality

$$1 + 2X + X^2 - 3h^2X \geq 0 \tag{3.21}$$

must hold. This means that for a chosen value of X the parameter h must obey

$$h^2 \leq \frac{(X + 1)^2}{3X}. \tag{3.22}$$

Solving equations (3.3), (3.14), and (3.19) or (3.20) we get

$$Y = \frac{8}{9} + \frac{8}{9}X \pm \frac{4}{9}U(X), \tag{3.23}$$

$$a = Z_1 \frac{X}{(h^2X + X^2 + 2X + 1)^{3/2} h}, \tag{3.24}$$

$$H = Z_2 \frac{1}{(h^2X + X^2 + 2X + 1)^{3/2} h}, \tag{3.25}$$

where U and Z_1, Z_2 are given by

$$U(X) = \sqrt{1 + 2X + X^2 - 3h^2X}, \tag{3.26}$$

$$Z_1 = \sqrt{w_1(X) \pm w_2(X)U(X)}, \tag{3.27}$$

$$Z_2 = \sqrt{w_3(X) \pm w_4(X)U(X)}, \tag{3.28}$$

$$w_1(X) = a_6X^6 + a_5X^5 + a_4X^4 + a_3X^3 + a_2X^2 + a_1X + a_0, \tag{3.29}$$

$$\left\{ \begin{array}{l} a_6 = 16h^2, \\ a_5 = 48h^4 + 96h^2, \\ a_4 = 48h^6 + 192h^4 + 240h^2 + 6\gamma^2, \\ a_3 = 16h^8 + 96h^6 + 288h^4 + (320 + 102\gamma^2)h^2 + 24\gamma^2, \\ a_2 = 48h^6 + 192h^4 + (162\gamma^2 + 240)h^2 + 36\gamma^2, \\ a_1 = (54\gamma^2 + 48)h^4 + (18\gamma^2 + 96)h^2 + 24\gamma^2, \\ a_0 = (16 - 42\gamma^2)h^2 + 6\gamma^2, \end{array} \right. \tag{3.30}$$

$$w_2(X) = b_3X^3 + b_2X^2 + b_1X + b_0, \quad (3.31)$$

$$\begin{cases} b_3 = 6\gamma^2, \\ b_2 = -51\gamma^2h^2 + 18\gamma^2, \\ b_1 = -9\gamma^2h^4 - 12\gamma^2h^2 + 18\gamma^2, \\ b_0 = 39\gamma^2h^2 + 6\gamma^2, \end{cases} \quad (3.32)$$

$$w_3(X) = c_7X^7 + c_6X^6 + c_5X^5 + c_4X^4 + c_3X^3 + c_2X^2 + c_1X + c_0, \quad (3.33)$$

$$\begin{cases} c_7 = -32h^2, \\ c_6 = -96h^4 - 192h^2, \\ c_5 = -96h^6 - 384h^4 - 480h^2 + 32Z_1h, \\ c_4 = -32h^8 - 192h^6 - 576h^4 + 64Z_1h^3 \\ \quad + (-640 - 42\gamma^2)h^2 + 128Z_1h + 6\gamma^2, \\ c_3 = -96h^6 + 32Z_1h^5 + (-384 + 54\gamma^2)h^4 \\ \quad + 128Z_1h^3 + (-480 + 18\gamma^2)h^2 + 192Z_1h + 24\gamma^2, \\ c_2 = 162\gamma^2h^2 + 64Z_1h^3 + 128Z_1h - 192h^2 + 36\gamma^2 - 96h^4, \\ c_1 = (102\gamma^2 - 32)h^2 + 32Z_1h + 24\gamma^2, \\ c_0 = 6\gamma^2, \end{cases} \quad (3.34)$$

$$w_4(X) = b_0X^3 + b_1X^2 + b_2X + b_3. \quad (3.35)$$

4. Analytical and numerical computations

Bifurcation diagram for the effective equation (2.11) is shown in Fig. 1 (colours mark different initial conditions) for the following values of control parameters $H = 0.04$, $h = 0.4$, $a = 0.8$, $\gamma = 2.5$.

Position of the 1 : 1 resonance agrees well with the amplitude profile, computed for the same parameters, *cf.* Fig. 2 and discussion in [8].

It follows from solutions obtained in the preceding section that we can control position of a singular point. More exactly, we choose a value of X and then h fulfilling inequality (3.22) can be chosen as well. Next we specify γ and then Y , a , H are computed from Eqs. (3.23), (3.24), (3.25). In this process the position of the singular point (X, Y) and values of control parameters H , h , γ , a are determined (provided that the solutions are real).

We shall now compute coordinates of a singular point using Eqs. (3.23), (3.24), (3.25). At first, we choose the value of X as $X = 9$ ($\Omega = 3$). Then, we can select any value of h obeying inequality (3.22). We thus put $h = 0.8$ to get from Eq. (3.19) $Y = 4.8466$ ($A = 2.2015$). Next, we choose $\gamma = 1.5$ to compute from (3.24), (3.25) $a = 9.0720$, $H = 0.2995$. In Fig. 3 we show

amplitude profiles computed from Eq. (3.1) for critical parameter values $(H, h, a, \gamma) = (0.2995, 0.8, 9.0720, 1.5)$, and for two more values of H , $H > H_{cr}$ and $H < H_{cr}$.

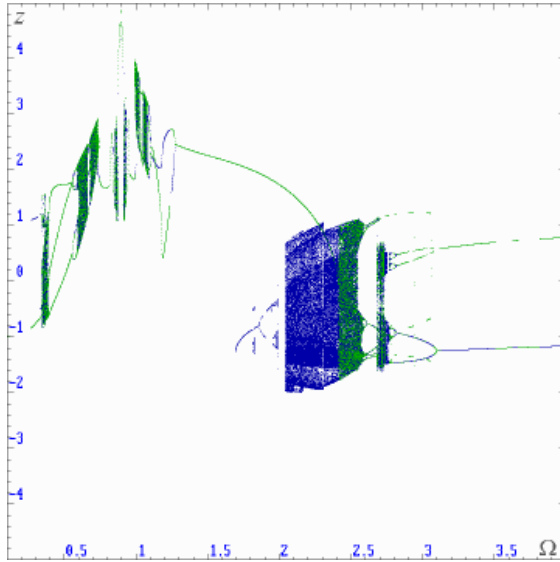


Fig. 1. Bifurcation diagram for Eq. (2.11), $h = 0.4$, $\gamma = 2.5$, $a = 0.8$, $H = 0.04$.

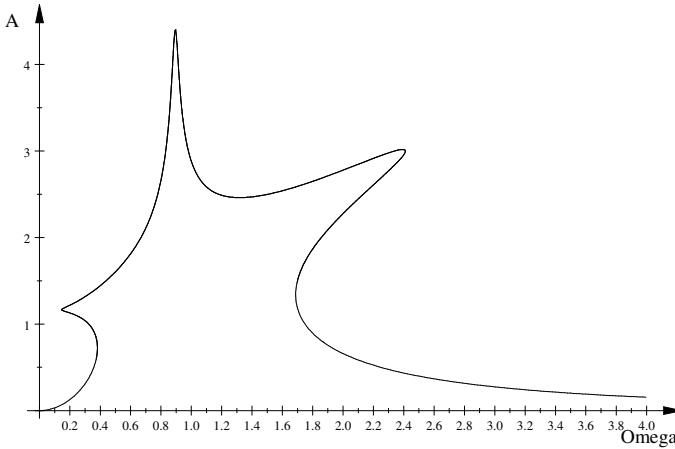


Fig. 2. Amplitude profile $A(\Omega)$, $h = 0.4$, $\gamma = 2.5$, $a = 0.8$, $H = 0.04$.

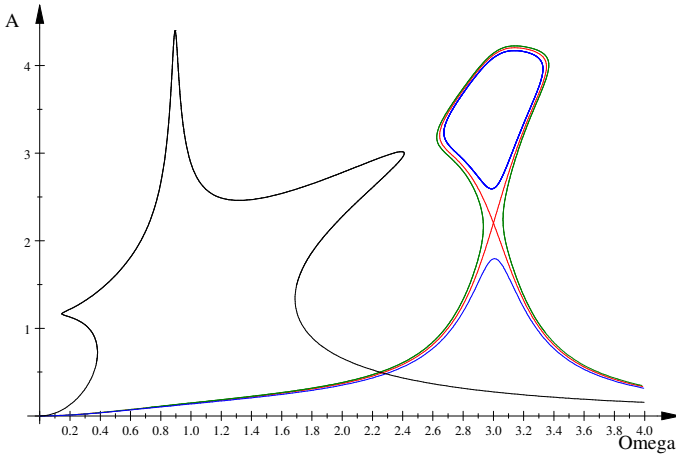


Fig. 3. $A(\Omega)$ in the singular point and in its neighbourhood, $h = 0.8$, $\gamma = 1.5$, $a = 9.0720$, and $H = 0.27$ (black/green), $H = 0.2995$ (grey/red), $H = 0.33$ (dashed/blue).

The critical (grey/red) curve intersects itself in singular point $(X, Y) = (4.8466, 9)$ or $(A, \Omega) = (2.2015, 3)$. Black (green) curve corresponds to $H = 0.27$ while dashed (blue) curve has been computed for $H = 0.33$ (other parameter values unchanged). The initial amplitude from Fig. 2 was also shown (black curve). The first bifurcation diagram, cf. Fig. 4, was computed for $H = 0.27$ and corresponds to the black (green) curve in Fig. 3. We note that the small branch of the 1 : 1 resonance is discontinuous in agreement with the amplitude profile shown in Fig. 3 (black/green curve).

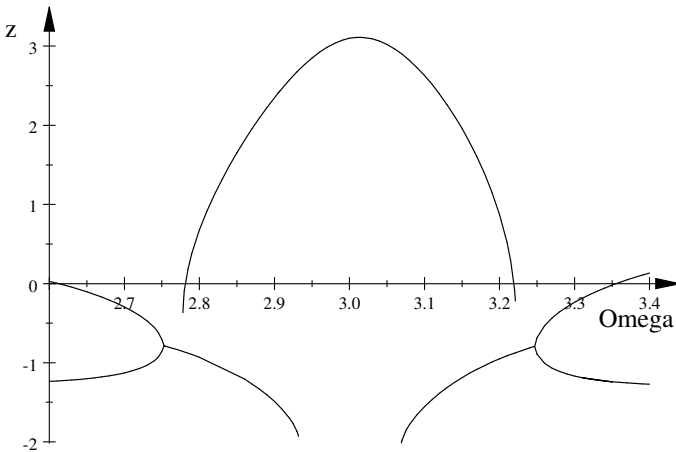


Fig. 4. Bifurcation diagram, $h = 0.8$, $\gamma = 1.5$, $a = 9.0720$, $H = 0.27$.

The next bifurcation diagram, Fig. 5, has been computed for critical value $H = 0.3019$ determined numerically from Eq. (2.11) (this differs slightly from the critical value $H = 0.2995$ determined from the KBM solution as described above).

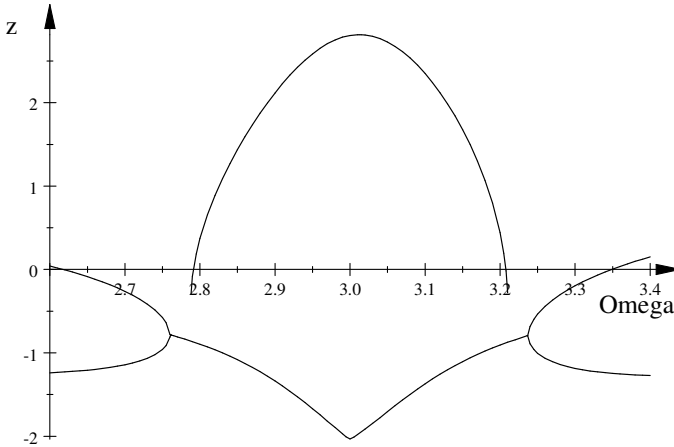


Fig. 5. Critical diagram, $h = 0.8$, $\gamma = 1.5$, $a = 9.0720$, $H = 0.3019$.

And finally, the last bifurcation diagram was computed for $H = 0.33$, and again the small branch of the 1 : 1 resonance is continuous, see Fig. 6.

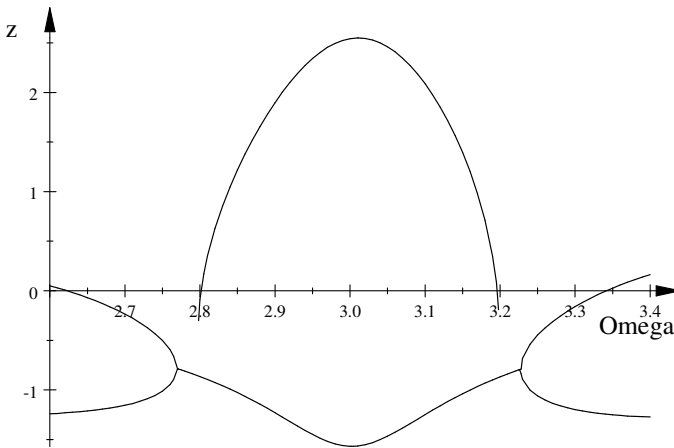


Fig. 6. Bifurcation diagram, $h = 0.8$, $\gamma = 1.5$, $a = 9.0720$, $H = 0.33$.

It follows from results presented in Sec. 3.2 that for $X = 9$, $h = 0.8$, $\gamma = 1.5$ there is another singular point. Indeed, we can compute Y from another equation (3.23) to get from Eqs. (3.24), (3.25) $Y = 12.9311$ ($A = 3.5960$), $a = 9.1213$, $H = 0.5158$.

In Fig. 7 amplitude profiles computed from Eq. (3.1) for critical parameter values $(H, h, a, \gamma) = (0.5158, 0.8, 9.1213, 1.5)$ and for two other values of H , $H < H_{cr}$ and $H > H_{cr}$ have been shown. Bifurcation diagrams for $H = 0.49$ and $H = 0.54$ are shown below.

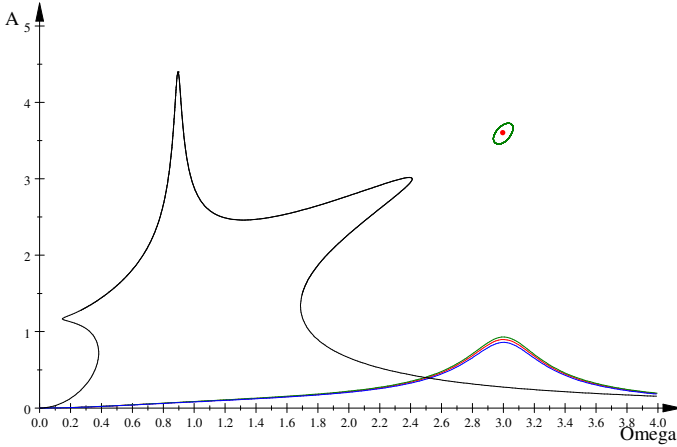


Fig. 7. $A(\Omega)$ in the singular point and in its neighbourhood, $h = 0.8$, $\gamma = 1.5$, $a = 9.1213$, and $H = 0.49$ (black/green), $H = 0.5158$ (grey/red, critical), $H = 0.54$ (dashed/blue).

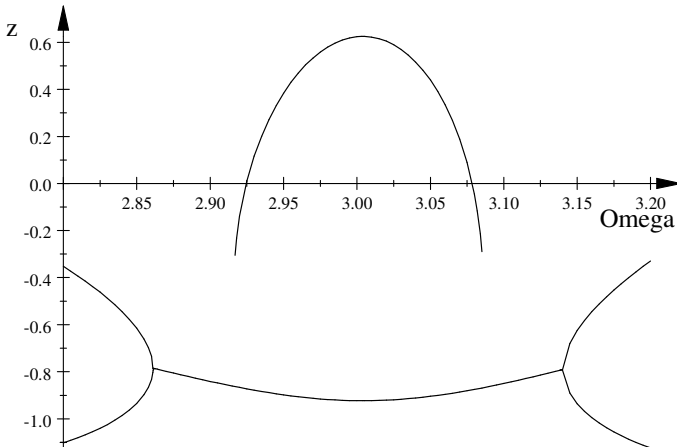


Fig. 8. Bifurcation diagram, $h = 0.8$, $\gamma = 1.5$, $a = 9.1213$, $H = 0.49$.

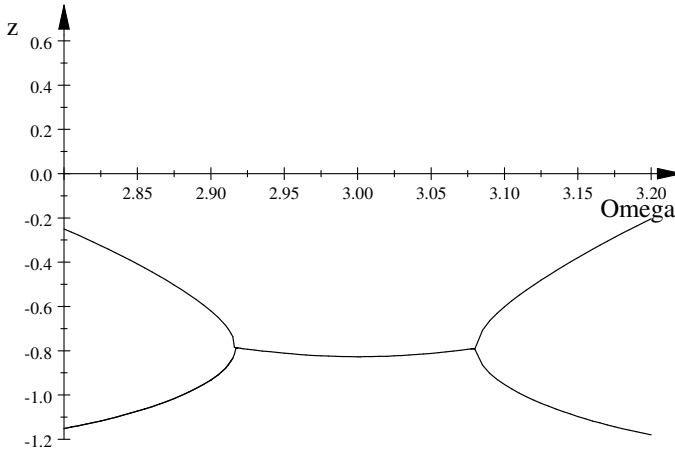


Fig. 9. Bifurcation diagram, $h = 0.8$, $\gamma = 1.5$, $a = 9.0720$, $H = 0.54$.

5. Summary and discussion

In this work we have studied metamorphoses of amplitude profiles for the effective equation, describing approximately dynamics of two coupled periodically driven oscillators. Our analysis has been analytical although based on the approximate KBM method.

Theory of algebraic curves has been used to compute singular points on effective equation amplitude profiles. It follows from general theory that metamorphoses of amplitude profiles occur in neighbourhoods of such points. In Section 3 we have computed analytically positions of singular points for the amplitude profiles $A(\Omega)$ determined within the Krylov–Bogoliubov–Mitropolsky approach for the approximate second-order effective equation (2.11). In the first case the singular point corresponds to self-intersection of $A(\Omega)$, see Fig. 3, while in the second case it is a isolated point, cf. Fig. 7.

It is interesting that the solution described in Sec. 3 permits control of position of singular point: we choose arbitrary value of variable X ($X^2 = \Omega$), then value of the parameter h obeying inequality (3.21) is selected. Finally, the value of the control parameter γ is chosen and Y , a , H are computed from Eqs. (3.23), (3.24), (3.25); it should be stressed that we have not come across any difficulties to obtain real solutions. We hope to carry full analysis of conditions guaranteeing existence of real solutions in our future papers. As a by-product we have demonstrated that there are no singular points for $A(\Omega)$ computed for the Duffing equation in agreement with well established numerical experience.

We have also computed numerically bifurcation diagrams in the neighbourhoods of singular points and indeed dynamics of the effective equation (2.11) changes according to metamorphoses of the corresponding amplitude profiles. It thus follows that control of position of the singular point permits control of dynamics.

In our future work we are going to study singular points of the amplitude profiles computed for the exact equation (2.8).

REFERENCES

- [1] W. Szemplińska-Stupnicka, *The Behavior of Non-linear Vibrating Systems*, Kluwer Academic Publishers, Dordrecht 1990.
- [2] J. Awrejcewicz, *Bifurcation and Chaos in Coupled Oscillators*, World Scientific, New Jersey, 1991.
- [3] J. Kozłowski, U. Parlitz, W. Lauterborn, *Phys. Rev.* **E51**, 1861 (1995).
- [4] K. Janicki, W. Szemplińska-Stupnicka, *J. Sound. Vibr.* **180**, 253 (1995).
- [5] A.P. Kuznetsov, N.V. Stankevich, L.V. Turukina, *Physica D* **238**, 1203 (2009).
- [6] J.P. Den Hartog, *Mechanical Vibrations*, 4th edition, Dover Publications, New York 1985.
- [7] S.S. Oueini, A.H. Nayfeh, J.R. Pratt, *Arch. Appl. Mech.* **69**, 585 (1999).
- [8] A. Okniński, J. Kyzioł, *Differential Equations and Nonlinear Mechanics* **2006**, Article ID 56146 (2006).
- [9] A.H. Nayfeh, *Introduction to Perturbation Techniques*, John Wiley and Sons, New York 1981.
- [10] J. Awrejcewicz, V.A. Krysko, *Introduction to Asymptotic Methods*, Chapman and Hall (CRC Press), New York 2006.
- [11] M. Spivak, *Calculus on Manifolds*, W.A. Benjamin, Inc., Menlo Park, California, 1965.
- [12] C.T.C. Wall, *Singular Points of Plane Curves*, Cambridge University Press, New York 2004.